Stability Control in Polygon Based Topology Formation and Information Gathering in Satellite Based Wireless Sensor Network

Padmaja Kuruba[1] · N. D. Dushyantha[2]

Abstract

The Space today has considerable surge in distributed network of small satellites to meet the imperative demand of both commercial and scientific applications (Selva and Krejci in Acta Astronaut 74:50–68, 2012). As the complexity of the design and launch of large satellites is high, the need of distributed networking is gaining lot of interest in space domain as well. Thus single large satellite is replaced by many, small satellite that collaboratively work to perform the same functionality of single large satellite forming Space Based Wireless Sensor Network (SBWSN). The SBWSN are dynamically decoupled network as each satellite, orbits in its own path and the positioned with considerable distance between them. Stability of network with respect to formation flying to accomplish the task by collaboration is quite essential. In this paper, we develop the stability criteria in small satellite network using graph theory, covariant derivatives and linear algebra to ensure distributed processing and communication, required to accomplish the mission task.

Keywords Small satellite network · Topology formation · Stability

1 Introduction

From last few years, small satellites are becoming predominant in space mission. These small satellites are built using well proven commercially off the shelf components (COTS) to reduce the mission time and increase reliability of the mission [1]. A lot of research is currently focused on replacing single large satellite using distributed network of small satellites to meet the increasing demand of the current generation. The application of SBWSN would be for earth observation like surveillance,

✉ Padmaja Kuruba
   padmajamtech@gmail.com

   N. D. Dushyantha
   dushyanthcrp@rediffmail.com

1 Department of Electronics and Communication Engineering, Global Academy of Technology, Bengaluru 560098, India

2 Department of Electronics and Communication Engineering, K S School of Engineering and Management, Bengaluru 560068, India

weather forecasting, cartography, military and agriculture. These can also be used for communication(satellite phones, TV), navigation (GPS, IRNSS), interplanetary exploration (Mars mission), deep space mission (path finder, magnetic field around earth, study of asteroids) etc.,. One more important aspect why space researchers are looking forward for SBWSN as it is the economically feasibility, increased life time, reduced development time & risk of mission failure. If one of the satellite fails the rest of the satellites in the network can adaptively reconfigure and continue the mission application.

Some of the challenges in SBWSN are (a) formation flying (b) collision between satellites or natural bodies in space, (c) Collaboration and coordination in the Network , (d) Node failure (e)Hardware/software resource constraints etc. In this paper, we focus on formation flying in small satellite network. The satellites in motion should follow predetermined trajectories for the defined topology to accomplish the mission task. This is what is known as formation flying in more general way. A basic requirement for any formation flying is to maintain the position of the satellite in the orbit. The bounded range of formation is, the line of sight of the satellites in formation. More precise definition of formation flying is given below.

Formation flying A group of satellites are said to be in formation flying if they maintain the relative distance between them with on-board control system. The satellites interact with each other, to maintain the formation of the satellites. There are several methods of implementation like (1) One leader and the rest are followers, where all the followers follow the leader as the reference, (2) The entire system of satellites in formation is controlled by a single satellite, (3) Each satellite takes their own measurements and later collaboratively realign to maintain the formation intact [2–4]

Formation flying depends on design parameters like launch orbit type, shape of the orbit, mass of satellites, number of satellites, swath, altitude control, orbital velocity, relative velocity, angular distance, orbital drift, drag, perturbation, solar radiation pressure, avoidance mechanism of orbital debris [5, 6]. It also depends on the satellite capabilities like frequency spectrum for communication and on-board data handling and control system, payload capabilities of temporal and spatial resolutions.

One of the major challenge in small satellite network is topology of the network and formation flying in space. Many researchers are now looking forward in control aspects of these formations in space. Further, formation flying is more complex in low earth orbit due to nodal regression because of flattened surface at the poles. With all these challenges, many small satellites forming a distributed network are still considered better than a single large satellite for its low cost, reduced development time and higher reliability. From the above discussion we see that formation dynamics plays a key role in realization of SBWSN.

In this work we discuss on formation flying control mechanism and determine the stability criteria for topology in SBWSN using graph theory and linear algebra. It provides stable interconnections possible in the network for sensing, communication and dynamic clustering in SBWSN. This work focus on decentralized control method, where formation is not controlled by a single dedicated satellite, instead all the satellites involve in control operation. These satellites in the network are decoupled physically, but coupled functionally by their task with distributed processing. The communication required for formation flying between the satellites is performed using inter satellite communication link (ISL). ISL requires line of sight (LOS) for communication. Therefore the satellites should be visible to each other for communication. This communication is essential for formation keeping of the satellites in space.

2 Related Works

From the literature the most widely used network in the space domain is the leader follower structure in which, one of the satellite/node is used as the leader while all the other nodes in the network are the followers. In this type of network, the leader determines its trajectory and the followers nodes takes leader as the reference and then align with the leader. The advantage of this formation is, its a simpler mechanism where only leader has more computation while the followers have less computational overhead. Thus the system is economical and less complicated. The disadvantage in this control mechanism is that, the failure of the leader results in the entire network failure which is not advisable in the distributed satellite network. [2]. The optimization of these are described by the author [7]. The author [8] in this works describe the use of decentralized mechanism to control the network formation where the nodes align in the decentralised form. The disadvantage is that all the nodes in the network should be equipped with required hardware and software which is little expensive. But its becomes advantages when compared to the mission cost that includes the launch of these nodes in the network. This also increases the reliability of the network and increases the life time of the network. The author [9] in their work have discussed about the advantages of small satellite network with respect to reliability and reduction of space debris which is caused due to large satellite when there is a mission failure. The importance of distributed network in space is described. Many Government and private space agencies are planning the distributed network of small satellites in future. The technology development in avionic industry has brought revolution in unmanned air vehicles has demonstrated the formation flying using small devices [2, 10]. The study of autonomous systems with dynamic control systems have proven the feasibility of having small satellites networks in space. Some of the control mechanisms used for optimal solution for the underlying dynamic system include mathematical modelling using lagrange system with levi civita connections, behaviour approach [11–13].

The author [14] has described about the network formation with mobile vehicles in distributed environment that work cooperatively which can adapt and reconfigure to the underlying environment based on artificial field potential. This helps us understand the strategy of the mobile nodes and its control mechanisms to optimise using adaptive gradient climbing method.

The author [15] describes, four models for Formation flying namely Ordinary Differential Equations expressed in terms of Cartesian coordinates (CODE), solution-based State Transition Matrix (STM) and Algebraic equations expressed in terms of Orbit Element Differences (OEDA). The author [16] describes State Dependent Riccati Equation (SDRE) for controlling the formation in a non linear system. These models help in determining the topology of the network. They also predict the capability of increasing the network size based on the relative distances and the corresponding error index in the formation. Each of these models have different accuracy and different bit error rate for different relative distance between satellites in the network. If the mission requires less computation then OEDA is used as it takes less computation time to solve differential equations on board.

From literature survey, we see space researchers are focusing on small satellites networks in place of one huge satellite. Some of the challenges in Satellite Based Wireless Sensor Network (SBWSN) [9, 17] are (1) Network topology, (2) Formation flying, (3) Dynamic reconfiguration during node failure, (4) Network reliability, (5) Processing capabilities and (6) Network Stability and Scalability. The proposed work focuses on formation flying and stability SBWSN.

2.1 Our Contributions

The main objective of this work is to determine the stability of the network topology in SBWSN. The topology under consideration is a distributed network formed by trivalent, toroidal and spherical polyhedron graph forming a fullerene. This topology is called as polygon based network topology (PBNT). The relative distance traversed by satellite at perigee is more, compare to satellite at apogee due to orbital parameters. Therefore, we cannot assume that the satellite moves at a constant speed at all time in space environment. Therefore we split the entire nodal period (time (T)) in time slices such that its derivative remains constant for that time slice. In this work, we focus on network trajectories and its stability control using time slicing, covariant derivative and linear algebra. Graph theory is used for network representation. This work also addresses the stability criteria in SBWSN for dynamic cluster formation and reconfiguration during node failure.

3 Proposed Work

The satellites are nothing but moving vehicles in space with certain motion dynamics. These dynamics are represented using the arc/trajectory of the movement in controlled manner using the covariant derivatives. One has to understand that the trajectory varies based on the topology of the network and underlying mechanical systems.

The scheme of operation in proposed work is described in the following steps (1) Design the topology of the Network (PBNT) with geometric parameters. (2) Determination of Time scaled Trajectories in SBWSN. (3) Position Determination using Vector space. (4) Graph theory representation of Network topology. (5) Stability of PBNT using linear algebra. (6) Validation using Nyquist plot.

3.1 Architecture of Network Topology in PBNT

We consider a distributed network formed by trivalent, toroidal and spherical polyhedron graph forming a fullerene, which is called as polygon based network topology (PBNT). It comprises of both pentagonal (F_p) and hexagonal (F_h) faces with K regular graphs such that $K \geq 3$ with genus equal to 1. It also satisfies Eulers formula with n vertices. The fullerene comprises of simple rings and each of this ring forms the cluster as shown in the Fig. 1a. Each cluster is further represented as a triangular grid as shown in the Fig. 1b, that is linearly convex or non-linear, with K-connected graph along with Hamiltonian extendible cycle [18]. A graph with hexagons is called as polyhex. Just for the purpose of representation we assume hexagons of same size, but in actual scenario the size of each hexagon(H) may vary based on the application. The polyhex is formed by H_n where $n = 1, 3, 4, 7, \ldots$ congruent hexagons. The skeleton of these polyhexes in planar graph with three fold tiling at the center is represented by black opaque dot, while the terminus is represented using a hallow circle. The Figs. 2 and 3 shows H_n for $n = 1, 3, 4, 7$. The center and the terminus helps in determining the formation of cluster required to cover a particular area of earth based on the application. These polyhexes form the logical cluster. The concept of tiling is used for dynamic clustering. The topology designed is a scalable and re-usable network using existing space infrastructure.
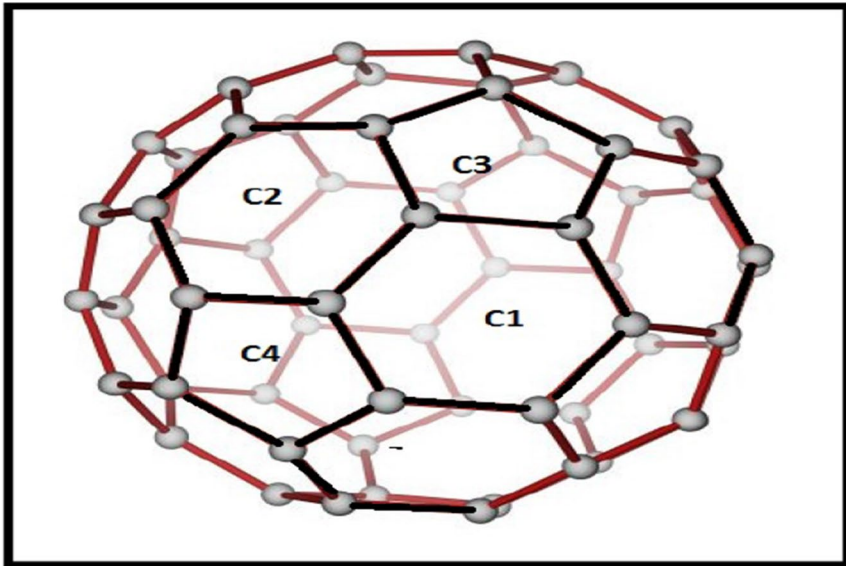
(a)
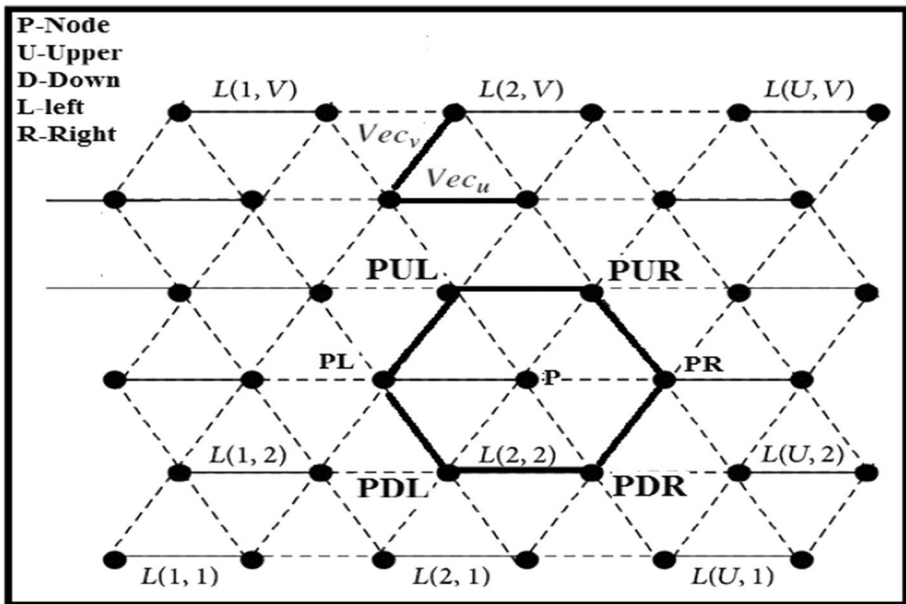
(b)

Fig. 1 a Geometrical framework of the PBTN and **b** triangular grid graph with adjacent nodes

Therefore maintaining formation flying of these satellites to its respective positions along the trajectories play a major role. Once the topology of the network is designed, the formation flying needs to determine the trajectories of these nodes [].
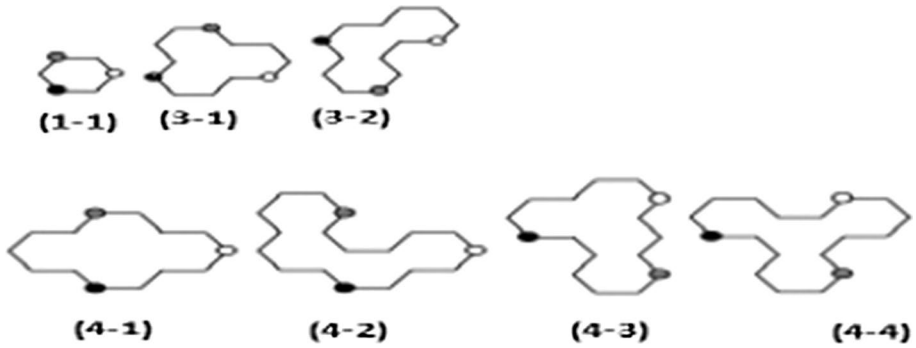
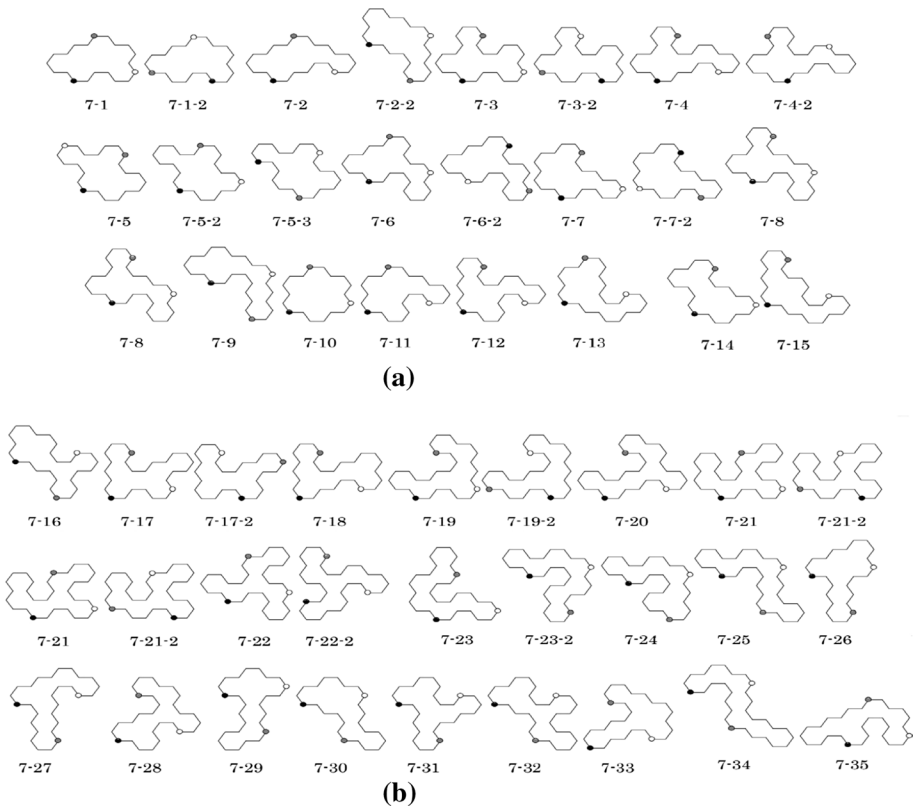**Fig. 2** Skeleton of polyhexes with its different inclination for n = 1–4

Fig. 3 Skeleton of polyhexes with its different Inclination for n = 7

3.2 Determination of Time scaled Trajectories in SBWSN

The entire time is spilt into small slices taking the advantage that the orbital dynamics of the satellite remains constant for a short interval of time forming a time scaled control system (TSCS). In the TSCS, we determine the trajectory from the initial-conditions at

time($t = t_i$) (i.e, current position) to the final position(i.e, desired position) at $t = t_f$ and is represented as $K(u)$ for the interval $t = (t_i, t_f)$, and $u(t)$ is the control history of the time scaled control system. We minimize this function $L(\hat{x}, u)$ for the control history u. Further by changing the coordinates of the integral and integrating over the time we get the expression 1

$$\int L(K(\hat{x}, v)) \, \alpha \, dt \tag{1}$$

Replace v by $k(u *)$ and using Jacobian transform, we see that $u = u *$ and $v = k(u *)$. Another important thing that we notice is $k(u *)$ is a compatible function which converges to the end point. Thus we get the variation from one time slice to other that helps in determining the maximum and minimum variation. The actual position and deviation is determined using optimal trajectory between the nodes in the network from x to y using vector space for curved surfaces with covariant derivatives. This gives the optimal solution for SBWSN.

3.3 Position Determination Using Vector space

In the normal network representation, the graph of the network is assumed to be in the flat surface and a simple distance formula would be sufficient to determine the adjacent nodes and the stability. Let us consider the example of the earth surface which is a sphere and the vectors to move from one point to another point as shown in the Fig. 4, the vector A and B cannot be same. If the Vector is considered as person at the pole while the vector B is on the equator, both are not same. Since the satellites orbit around the earth which is an oblate spheroid, we cannot use the flat surface vector space analysis. Therefore we use curved space
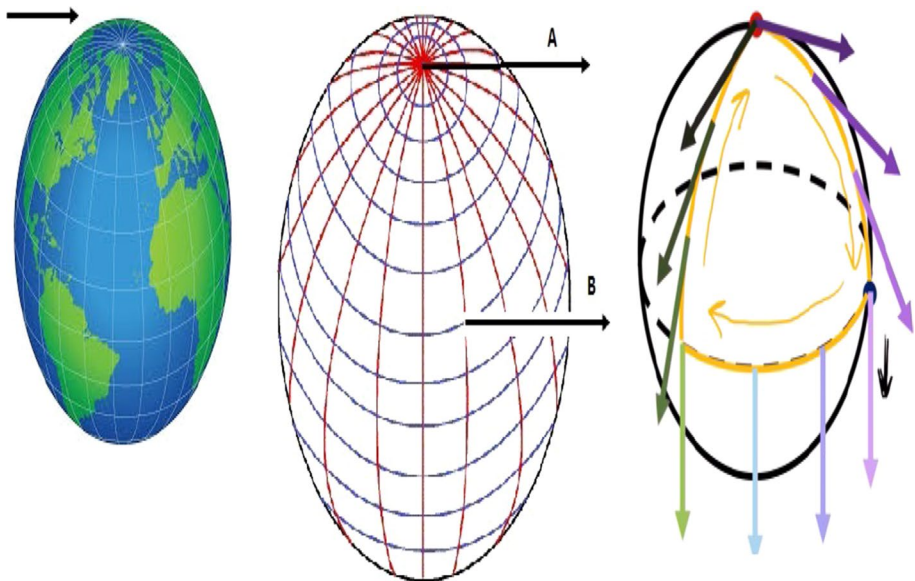

Fig. 4 Example of vector movement on the earth surface

for determining path, adjacent nodes and formation stability. we use a method of transporting geometrical data, along smooth curves in a manifold. The two vectors on the sphere are identical or different are determined using the path of the nodes. The path of the node is determined using the rate of change(ROC) of the vector, but the rate of change of vector on the sphere when taken in small steps are normal to the surface of the curve and expressed by the following Eq. 2.

$$\frac{d\vec{v}}{d\lambda} = \vec{n} \tag{2}$$

$\vec{n}$ is normal vector to ROC. Thus variation from position along the path of the satellites is obtained using covariant derivatives ($\nabla_{\vec{w}}\vec{v}$). Further subtract normal from the ROC vector-field ($\vec{v}$) in the direction of ($\vec{w}$) as given in the Eq. 3.

$$\nabla\frac{d\vec{v}}{d\lambda} = \frac{d\vec{v}}{d\lambda} - \vec{n} \tag{3}$$

It is always easier to understand and analyse 2D plane than 3D plane. Hence we transform 3D plane to 2D plane where $pu1$, $pu2$ plane represent the 2D surface of a sphere and is shown in the Fig. 5.

Any vector on sphere in curved surface with (x, y, z) coordinates are represented by the following expressions 4, 5, 6 and 7.

$$\vec{R} = (X(pu1, pu2), Y(pu1, pu2), Z(pu1, pu2)) \tag{4}$$
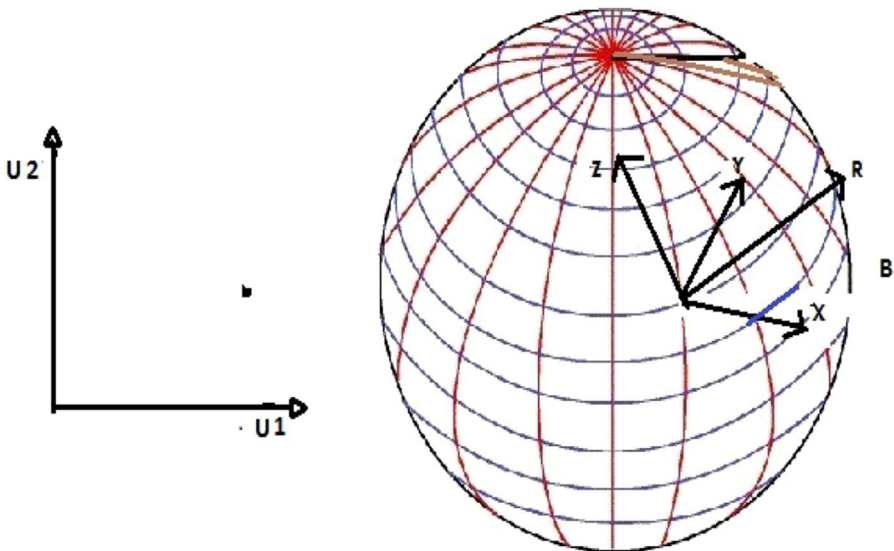
$$x = cos(pu1)sin(pu2) \tag{5}$$

Fig. 5 Example of vector movement on the earth surface

$$y = sin(pu1)sin(pu2) \tag{6}$$

$$z = cos(pu2) \tag{7}$$

$$\vec{e1} = \frac{d\vec{R}}{dpu1} \tag{8}$$

$$\vec{e2} = \frac{d\vec{R}}{dpu2} \tag{9}$$

where $pu1$ *and* $pu2$ are the longitudes and latitudes respectively and $\vec{e1}, \vec{e2}$ are the basis functions for the covariant derivatives along $pu1$ *and* $pu2$. These are the tangents for curves respectively. The covariant derivatives of the tangent vector field in the direction of pu_i is represented as $\nabla \frac{d\vec{v}}{dpu_i}$ which are the normal derivatives but subtracted by the normal vector and shown by the Eq. 10. The Eq. 11 is written as a linear combination of the vectors.

$$\nabla \frac{d\vec{v}}{dpu_i} = \frac{d\vec{v}}{dpu_i} - \vec{n} \tag{10}$$

$$= \left(\frac{d}{dpu_i} [v1\vec{e}_1 + v2\vec{e}_2] \right) - \vec{n} \tag{11}$$

$$= \left(\frac{d}{dpu_i} \sum_j v_j \vec{e}_j \right) - \vec{n} \tag{12}$$

$$using\ product\ rule \tag{13}$$

$$= \left(\frac{d\vec{vj}}{dpu_i} \vec{e}_j + \vec{vj} \frac{d\vec{e}_j}{dpu_i} \right) - \vec{n} \tag{14}$$

We know that $\frac{d\vec{e}_j}{du_i}$ is the derivative of basis vector and can be written as the linear combination as shown in the Eq. 15.

$$\frac{d\vec{e}_j}{dpu_i} = \Gamma^1 \vec{e}_1 + \Gamma^2 \vec{e}_2 + L_{ij}\vec{n} \tag{15}$$

$$taking\ summation \tag{16}$$

$$= \sum_k \Gamma^1 \vec{e}_k + L_{ij}\vec{n} \tag{17}$$

L_{ij} are the components of normal vector and substituting the 17 in Eq. 14, We get 18

$$\left(\frac{d\vec{vj}}{du_i} \vec{e}_j + \vec{vj} \, (\, \Gamma^k \vec{e}_k + L_{ij} \vec{n}) \right) - \vec{n} \tag{18}$$

Changing variable and taking the normal vector outside, we get the following Eq. 19. The tangent plane is formed using tangent basis shown in Eq. 20 and further normal component vanishes, as the normal is also normal to the tangent space formed by the basis and finally we obtain the covariant derivative as in Eq. 20

$$\nabla \frac{d\vec{v}}{dpu_i} = \left(\frac{d\vec{vk}}{dpu_i} \vec{e}_k + \vec{vj} \, (\, \Gamma^k \vec{e}_k) \right) + L_{ij} \vec{n} - \vec{n} \tag{19}$$

$$\nabla \frac{d\vec{v}}{dpu_i} = \left(\frac{d\vec{vk}}{dpu_i} + \vec{vj} \Gamma^k \right) \vec{e}_k \tag{20}$$

Taking the dot product with a tangent vector of the Eq. 21 we obtain the metric tensor component 22.

$$\frac{\vec{e}_j}{du_i} \dot{\vec{e}}_l = \Gamma^k \vec{e}_k \dot{\vec{e}}_l \tag{21}$$

$$= \Gamma^k g_{kl} \tag{22}$$

Where g_{kl} are the metric tensor. We don't want to have the metric tensor component hence we can use a inverse tensor metric to get the δ which is defined as follows

$$\delta_k^m = \begin{cases} 1, & \text{if } (m = k) \\ 0 & \text{Otherwise} \end{cases} \tag{23}$$

$$\frac{\vec{e}_j}{du_i} \dot{\vec{e}}_l g_{lm} = \Gamma^m \delta_k^m \tag{24}$$

$$= \Gamma^m \delta^m \tag{25}$$

3.3.1 Determine Tangent Basis Vector

The partial derivatives of the (x, y, z) in Eqs. 5, 6, 7 are used to determine the tangents in terms of $pu1$ and $pu2$. A multivariable chain rule is applied to obtain the following Eqs. 26 to 29

$$\frac{d\vec{R}}{dpu_1} = \frac{d\vec{X}}{dpu_1} \frac{d\vec{R}}{dpu_X} + \frac{d\vec{Y}}{dpu_1} \frac{d\vec{R}}{dpu_Y} + \frac{d\vec{Z}}{dpu_1} \frac{d\vec{R}}{dpu_Z} \tag{26}$$

$$\frac{d\vec{R}}{dpu_1} = \frac{d\vec{X}}{dpu_2} \frac{d\vec{R}}{dpu_X} + \frac{d\vec{Y}}{dpu_2} \frac{d\vec{R}}{dpu_Y} + \frac{d\vec{Z}}{dpu_2} \frac{d\vec{R}}{dpu_Z} \tag{27}$$

$$\frac{d\vec{R}}{dpu_1} = cos(pu2)cos(pu1)\frac{d\vec{R}}{dX} + sin(pu2)cos(pu1)\frac{d\vec{R}}{dY} - sin(pu1)\frac{d\vec{R}}{dZ} \qquad (28)$$

$$\frac{d\vec{R}}{dpu_2} = -sin(pu2)cos(pu1)\frac{d\vec{R}}{dX} + cos(pu2)sin(pu1)\frac{d\vec{R}}{dY} \qquad (29)$$

$\frac{d\vec{R}}{dpu1} \cdot \frac{d\vec{R}}{dpu2}$ We further get the tensor matrix using dot product as shown in the Eqs. 30 and 31 and inverse is obtained using Eq. 32

$$g_{ij} = \begin{bmatrix} \frac{d\vec{R}}{dpu1} \cdot \frac{d\vec{R}}{dpu1} & \frac{d\vec{R}}{dpu1} \cdot \frac{d\vec{R}}{dpu2} \\ \frac{d\vec{R}}{dpu2} \cdot \frac{d\vec{R}}{dpu1} & \frac{d\vec{R}}{dpu2} \cdot \frac{d\vec{R}}{dpu2} \end{bmatrix} \qquad (30)$$

$$= \begin{bmatrix} 1 & 0 \\ 0 & (sin(pu1))^2 \end{bmatrix} \qquad (31)$$

$$Inv\ of\ g_{ij} = \begin{bmatrix} 1 & 0 \\ 0 & \frac{1}{(sin(pu1))^2} \end{bmatrix} \qquad (32)$$

Substituting $\frac{d\vec{R}}{dpu1} = \vec{e}_i$ we get Eq. 33 and similarly we obtain for all the coordinates as shown in the Eqs. 34 to 38

$$\frac{d}{dpu1}\left(\frac{d\vec{R}}{dpu1}\right) = -cos(pu2)sin(pu1)\frac{d\vec{R}}{dX} - sin(pu2)sin(pu1)\frac{d\vec{R}}{dY} - cos(pu1)\frac{d\vec{R}}{dZ} \qquad (33)$$

$$\frac{d}{dpu1}\left(\frac{d\vec{R}}{dpu1}\right) = - cos(pu2)sin(pu1)\vec{e_X} - sin(pu2)sin(pu1)\vec{e_Y} - cos(pu1)\vec{e_Z} \qquad (34)$$

$$\frac{d}{dpu2}\left(\frac{d\vec{R}}{dpu2}\right) = - cos(pu2)sin(pu1)\frac{d\vec{R}}{dX} - sin(pu2)sin(pu1)\frac{d\vec{R}}{dY} \qquad (35)$$

$$\frac{d}{dpu2}\left(\frac{d\vec{R}}{dpu2}\right) = - cos(pu2)sin(pu1)\vec{e_X} - sin(pu2)sin(pu1)\vec{e_Y} \qquad (36)$$

$$\frac{d}{dpu1}\left(\frac{d\vec{R}}{dpu2}\right) = - sin(pu2)cos(pu1)\frac{d\vec{R}}{dX} + cos(pu2)cos(pu1)\frac{d\vec{R}}{dZ} \qquad (37)$$

$$\frac{d}{dpu1}\left(\frac{d\vec{R}}{dpu2}\right) = - sin(pu2)cos(pu1)\vec{e_X} + cos(pu2)cos(pu1)\vec{e_Z} \qquad (38)$$

From this we calculate the Γ^2 using the dot product as given by the Eqs. 39 to 46

$$\Gamma_{11}^1 = \left(\frac{d\vec{e}_1}{dpu1} \cdot \vec{e}_l\right) g^{l1} \tag{39}$$

$$\Gamma_{12}^1 = \left(\frac{d\vec{e}_2}{dpu1} \cdot \vec{e}_l\right) g^{l1} \tag{40}$$

$$\Gamma_{21}^1 = \left(\frac{d\vec{e}_1}{dpu2} \cdot \vec{e}_l\right) g^{l1} \tag{41}$$

$$\Gamma_{22}^1 = \left(\frac{d\vec{e}_2}{dpu2} \cdot \vec{e}_l\right) g^{l1} \tag{42}$$

$$\Gamma_{11}^2 = \left(\frac{d\vec{e}_1}{dpu1} \cdot \vec{e}_l\right) g^{l2} \tag{43}$$

$$\Gamma_{12}^2 = \left(\frac{d\vec{e}_2}{dpu1} \cdot \vec{e}_l\right) g^{l2} \tag{44}$$

$$\Gamma_{21}^2 = \left(\frac{d\vec{e}_1}{dpu2} \cdot \vec{e}_l\right) g^{l2} \tag{45}$$

$$\Gamma_{22}^2 = \left(\frac{d\vec{e}_2}{dpu2} \cdot \vec{e}_l\right) g^{l2} \tag{46}$$

From the above calculation we see that $\Gamma_{11}^1 = \Gamma_{12}^1 = \Gamma_{21}^1, \Gamma_{11}^2, \Gamma_{22}^2 = 0$; and $\Gamma_{12}^2, \Gamma_{22}^2$ is given by the Eqs. 47 and 48

$$\Gamma_{12}^2 = \Gamma_{21}^2 = \frac{cos(pu1)sin(pu1)}{sin(pu1)^2} = \frac{cos(pu1)}{sin(pu1)} = cot(pu1) \tag{47}$$

$$\Gamma_{22}^1 = (-cos(pu1)sin(pu1))(1) = -\left(\frac{1}{2}sin(2x)\right) \ as \ sin(2x) = 2cos(x)sin(x) \tag{48}$$

Finally covariant derivatives obtained are 49 and 50

$$\nabla \vec{e}_1 \vec{v} = \left[\frac{v^2}{dpu1} + v^2 cot(pu1)\right] \vec{e}_2 \tag{49}$$

$$\nabla \vec{e}_2 \vec{v} = \left[\frac{v^2}{dpu2} - v^2 - \frac{1}{2}sin(2u1)\right] \vec{e}_1 + \left[\frac{v^2}{dpu2} + v^1 cot(pu1)\right] \vec{e}_2 \tag{50}$$

From the above method we derive the covariant derivatives of the nodes which is further used to determine the distance between them. These covariant derivatives provide us the connection between the tangent space in the curved surface using parallel transport. Thus

the connection between the nodes at different time is calculated to determine the deviation from the required position.

3.4 Network Architecture Using Graph Theory

The easy way to represent SBWSN architecture is by using graph. SBWSN comprises of a geometric structure based topology. The nodes/vertices(V) in the graph represent the satellites and the edges E represent the interconnection between the satellites. They are bidirectional. They also determine which nodes are in communication range and in line of sight. It is essential that every node should be in the close proximity of at least one node at any given time.

Since we are discussing the small satellites for earth observation the satellite network is assumed to be in low earth orbit. This can be further extended to any orbit based on the mission application. The graph G is represented by the following Eq. 51

$$G = (V, E) \tag{51}$$

Where $V = (v_1, v_2 \ldots)$, $E = (u_{xy})$ edges connect adjacent vertices. We use weighted graph representation $w : V * V - R$ such that $w(u, v) = w(v, u)$ and $w(u, v) >= 0$, else the node is said to be isolated node if the node does not have a path joining any other node in the network as given by the Eq. 53. If every node is connected to every other node in the network, then such graphs are known as strongly connected graphs and the graphs are complete [19]. In this work we assume that each node is connected to one or more nodes in the graph with different incoming and outgoing paths. The number of incoming paths and outgoing paths are termed as in/out degree of the node. The degree of node is defined by the Eq. 52

$$d_v = \sum w(v, u) \text{ or } w(u, v) \tag{52}$$

The general representation is given by the Eq. 53

$$L(u, v) = \begin{cases} d\{v\} = w(u, u), & \text{if } (v = u) \\ w(u, v) & \text{if } (nodes\ u\ and\ v\ are\ adjacent), \\ 0 & \text{Otherwise} \end{cases} \tag{53}$$

This can further be represented as a function by the Eq. 54

$$L(f(x)) = \sum f(x) - f(y)w(x, y) \tag{54}$$

where x, y in the graph represent the connections between the nodes in the matrix-form, using algebraic graph concepts.

These graphs can further be contracted where two nodes u and v can be replaced by $v *$ as, weights of $v *$ is given by the Eqs. 55 and 56

$$w(x, v *) = w(x, v) + w(x, u) \tag{55}$$

$$w(v *, v *) = w(u, u) + w(v, v) + 2w(u, v) \tag{56}$$

As the nodes move, there is a possibility that not all the nodes in the network are connected all the time. It is always suggestibility to have a subset of the graph G, such that there exists one or more edges getting connected to the vertex of the node connected to outside vertices

not belonging to that subset. These form subgraphs. The subgraphs may have single pen-
dent vertex or more. The concatenation of subgraphs form the dynamic clusters used to
cover a specific swath of earth. The subgraphs are shown in the Fig. 6. These nodes are
measured for connectivity between them using existence of path between the nodes. The
Laplacian matrix is used in our work to determine the connected nodes using tangent basis
[20]. We further use Frobenius' theorem which gives many independent solutions for the
linear system of nodes and partial differential equations. This basically provides equiva-
lence connection in the manifold which is formed by a set of tangent vector basis function.
The distance between them is determined by the Laplacian matrix.

Laplacian Matrix (L) is simple matrix which represents the graph into a matrix. This
matrix is commonly used to determine eigenvalue and eigenvector that form independent
solution for linear systems [21–23]. Laplacian matrix is defined by the Eq. 57

$$L = D - A. \tag{57}$$

where D indicates out-degree or in-degree of the graph and A indicates adjacency matrix.
Further the laplacian matrix helps in understanding the discrete/continuous representations
in graph and vector spaces. This optimises the given network interconnections for com-
munication distance, delay and fuel efficiency. we now determine the eigen values of lapla-
cian matrix which is essential to determine if these trajectories are stable in their formation
using Linear algebra.

The spectral graph theory is a key for understanding the graph properties using eigen
value and eigen vectors.Form the above we know the graph that has vertices and edges
forming the topology of the network [21]. As we understand that the given network under
consideration is on the sphere which is a 2D surface the distance between them cannot be
directly a scalar entity. This also involves the vector representation. In the next section we
describe the time scaling method to determine the position of the node in the orbit(curved
surface) with time slicing method

3.4.1 Stability of SBWSN Using Linear Algebra

One of the major concepts in linear algebra is the eigenvalues. These eigenvalues are associ-
ated in determining the stability of graphs. L is nothing but normalised version of matrix A.
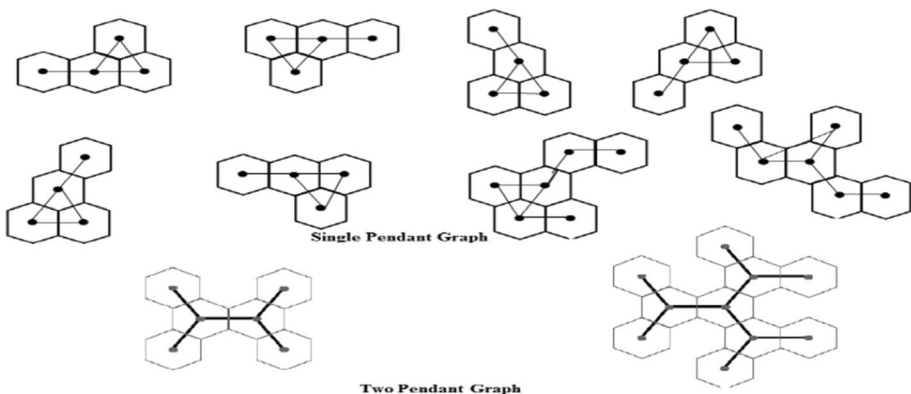

Fig. 6 Subgraphs and its concatenation forming clusters

We take the characteristic equation and find the roots of these characteristic equation known as eigenvalues. These are taken along the diagonal of the L matrix. Zero is always a eigenvalue ($\sum (xi - xj)^2 = 0$). The eigenvalue with multiplicity of Zero is equal to the number of components/interconnections in spectral graph. It also shows the algebraic connectivity $\lambda_1 = 0 <= \lambda_2 <= \lambda_n$. More connectivity is found for larger value of λ_2. From this we can determine the number of components/connectivity in the graph, at any given time slice. The communication components determine the neighbourhood set required for formation keeping, dynamic clustering and information gathering.

The structural properties and stability of the network is defined by laplacian matrix and eigenvalue. The network is stable if all the eigenvalues(non zero) lies in disk radius of 1 that are usually having uniform spacing between them (strongly connected graphs). The strongly connected graph lies within the disk radius 1 on the gregorian disc boundary for aperiodic graph and for periodic graph lies on the boundary of angular spacing of 2pi/M Gregorian disc.

The clusters are also formed by forming the sub-graphs which is very much required in SBWSN. These also help in scalability or reconfiguration during node failure specially when there are no edges between the connected nodes. These problem of instability is further addressed by using Cheegers inequality which puts extension of lower bound and upper bound of the graph. This also devices the use of graph theory concepts in redetermining the graph bounds and establishing the formation in the SBWSN.

3.5 Mathematical Model for Formation Stability in PBNT

In this section we deal with the formation and finding the stability of these small satellite network. Let us consider a group of nodes N, where $N = i, j$, where $((i, j) = 1, 2, 3, \ldots)$. Let N_i and N_j be the two satellites that are trying to involved in determining the nearest neighbour possibility to interconnect. The node N_{ij} is said to be in the formation if their exists a path between atleast with one another node. The linear dynamics of vehicular motion is given by Eq. 59

$$p.i = Api + Bqi \tag{58}$$

$$qi = C1pi \tag{59}$$

The relative distance information between the nodes is determined by the Eq. 60

$$rij = C2(qi - pi)j \in Mi \tag{60}$$

pi indicates state vector, $i = 1, 2, \ldots$, qi represent internal state and rij represents local state/external state of satellite in the network and Mi set of nodes that can locate the other nodes in the network. The deviation or error in the node is given by Eq. 61

$$e_i = \frac{1}{M_i} \sum_{j=1}^{M_i} r_{ij} \tag{61}$$

Using the state space method and decentralised control law, we map q_i and r_i to pu_i as given in the equation

$$\dot{v}_i = K_A v_i + K_{B1} qi + K_{B2} ri \tag{62}$$

$$p\dot{u}_i = K_C v_i + K_{D1} qi + K_{D2} ri \tag{63}$$

Let us consider the source and destination nodes in the network being represented by the matrix 64 and matrix 65. The connectivity are now put in the matrix form. The matrix entry has a value if their exists a edge between the nodes, else the value is zero.

$$SrcNodes = \begin{bmatrix} a11 & a12 & \cdots & a1q \\ a21 & a22 & \cdots & a2q \\ a31 & a32 & \cdots & a3q \\ \vdots & \vdots & \vdots & \vdots \\ am1 & am2 & \cdots & mq \end{bmatrix} \tag{64}$$

$$DestNodes = \begin{bmatrix} b11 & b12 & \cdots & b1p \\ b21 & b22 & \cdots & b2p \\ b31 & b32 & \cdots & b3p \\ \vdots & \vdots & \vdots & \vdots \\ bn1 & bn2 & \cdots & bnp \end{bmatrix} \tag{65}$$

The matrix 66 shows the communication link and corresponding distance between source and destination nodes.

$$Distance\_between\_Nodes = \begin{bmatrix} a11b11 & a12b11 & \cdots & a1nb11 \\ a11b21 & a12b12 & \cdots & a1nb12 \\ \vdots & \vdots & \vdots & \vdots \\ a11bm1 & a12bm2 & \cdots & a1nbmn \end{bmatrix} \tag{66}$$

This is further represented as sum of $A \otimes I + I \otimes B$ similarly A can be written as $A \otimes I$ when A is matrix that repeats along the diagonal. Thus the entire formation can be written as using standard system dynamics

$$\dot{x} = \hat{P}_A x + \hat{P}_B \hat{K}_{D_1} \hat{P}_{C1} x + \hat{P}_B \hat{K}_{D_2} \hat{P}_{C_2} L_n x + \hat{P}_B K_{C_v} \tag{67}$$

$$\dot{v} = \hat{K}_A v + \hat{K}_{B_1} \hat{P}_{C_1} x + \hat{K}_{B_2} \hat{L}_n x. \tag{68}$$

The correction required for each of the node varies with respect to the basis function, and it becomes essential for all the nodes to have the same basis function, we use Schur transformation and Jorden decomposition for transforming the basis function such that the oblique projections have an equivalent orthogonal projections using the expansion or the contraction of the positions required for having proper correction factor for each individual nodes which is applicable for all the nodes in the network. Thus Eigen vectors and Eigen values are these factors which determine the projection and the factor of expansion or contraction required for basis function during transformation. There are many ways to find the eigenvalues. One such method is QR method. The QR method finds eigenvalues for real or complex matrices as given by the Eq. 69

$$P^k = Q_k R_k \tag{69}$$

where Q_k is similar transform as P_k of using orthogonality and upper triangular matrix, though the convergence in most of the times is guaranteed but involves lot of iterations.

Therefore, we use the schur transform in this paper for decomposing the Laplacian matrix which can have several subsets of the network. This is helps in dynamic cluster formation. The schur decomposition is defined as matrix decomposition where an arbitrary matrix can be decomposed in to unitary matrix to an upper triangular matrix, where its eigen values represent the diagonal elements of the actual matrix.

Let P be a matrix where $P \in C^{n*n}$ and schur decomposition is given by equation

$$P = QUQ^* \tag{70}$$

where Q represents unitary matrix and * indicates its hermitian transpose $m * n$ matrix. From the fundamental of linear algebra we know that QQ^* is a Identity matrix and the roots of these characteristic polynomials always lie along the diagonal of the matrix. If the matrix are real then Jacobi Transform would be used, if the matrix are complex then schur decomposition is used. Schur decomposes the P invariant subspaces $0 = V_0 \subset V_1 \subset V_2 \subset V_3 \cdots \subset V_n = C^n$ where an orthonormal basis exists, such that for i basis vectors spans only V_i for every i, that occurs in nested sequence which stabilizes the complex N dimensional vector space $(V_0, V_1, V_2 \ldots V_n)$.

In our work we assume each of the basis vector as a matrix which hold only a subset of nodes from the entire set of nodes in the network. Thus we have chosen this transform for determining the stability of the network. The stability of the upper triangular matrix of the schur decomposition which has eigenvalue to be stable if the entire system has to be stable. From the above schur transformation we have decomposed the entire network into subsets which are nested in the vector space with the eigenvalues and vectors that either compress or expand the vector space(i.e. Maximizing the minimum eigenvalue/ Minimizing the maximum eigenvalue/ Minimizing the spectral norm) to obtain the optimal solution.

In linear algebra system the given matrix A is stable iff all the eigenvalues of the matrix have $norm(A) < 1$ (i.e, $\rho(A) < 1$). This means the relative equilibrium point is stable for all the nodes in the formation. In other words the trajectories should decrease to zero for the system to be stable .

In SISO system we determine the stability by the encirclements of the $-\lambda_i^{-1}$ is zero by plotting a Nyquist plot for all values $\lambda_i \neq 0$ by the forward loop = Number of poles = 0. The mimo system(P(s) stability for network formation is stable if $\rho(C(j\omega)) < M^{-1}$ where $-\infty < \omega < \infty$. We can determine the stability of the system for the given topology with the relative distance and visibility of the nodes for formation. These can also be further optimised by minimizing the eigenvalues using minimization techniques. This shows that stability of the system is controller by the diagonal elements shown by the Eqs. 72 to 73.

$$\dot{p} = P_A p + P_B u \tag{71}$$

$$q = P_{C_i} p \tag{72}$$

$$Z = \lambda_i P_{C_i} p \tag{73}$$

4 Results

The topology of the network should be determined for proper formation of the network. Therefore its important to determine the stability of the network topology. In this work, we have designed a distributed network topology of small satellites formed by trivalent, toroidal and spherical polyhedron graph forming a fullerene, which is called as polygon based network topology (PBNT). It comprises of both pentagonal (F_p) and hexagonal (F_h) faces with K regular graphs such that $K \geq 3$ with genus equal to 1. It also satisfies Eulers formula with n vertices. The fullerene comprises of simple rings and each of this ring forms the cluster as shown in the Fig. 7.

Each cluster is further represented as a dtriangular grid, that is linearly convex or nonlinear, with K-connected graph along with Hamiltonian extendible cycle. If one the pentagon/Hexagon is determined then rest of the fullerence is determined in the same way. Let us consider one pentagon of a PBNT, the vertex are the nodes while the edges are the communication links between the nodes as described by the Eq. 51. In this work, the simulation is done using matlab and results are discussed in the two steps.

- Firstly, Simulate triangular formation of the satellite trajectory/Path with vertical planar locations.
- Secondly, Determine the stability of Pentagon and Hexagon Graph.

In the first scenario, we consider two satellites and determine the trajectory of the satellite in the vertical planar location. The satellite are said to be in the formation if the position of two satellites align to the required position and proper angular velocity. Later we are using the triangular gird formation scenario in the topology, three satellites in triangular formation is simulated. The angular distance, speed and velocity determine satellite-position in the network. The deviation of these parameters from the actual and obtained determine the position of the satellites in the network and is shown by the Fig. 8. In formation flying each satellite in the network determines its position with its neighbour. Thus the deviation with respect to position and velocity is determined
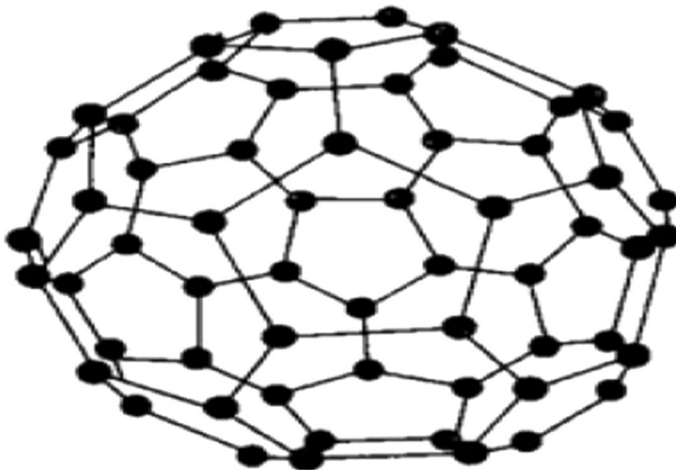

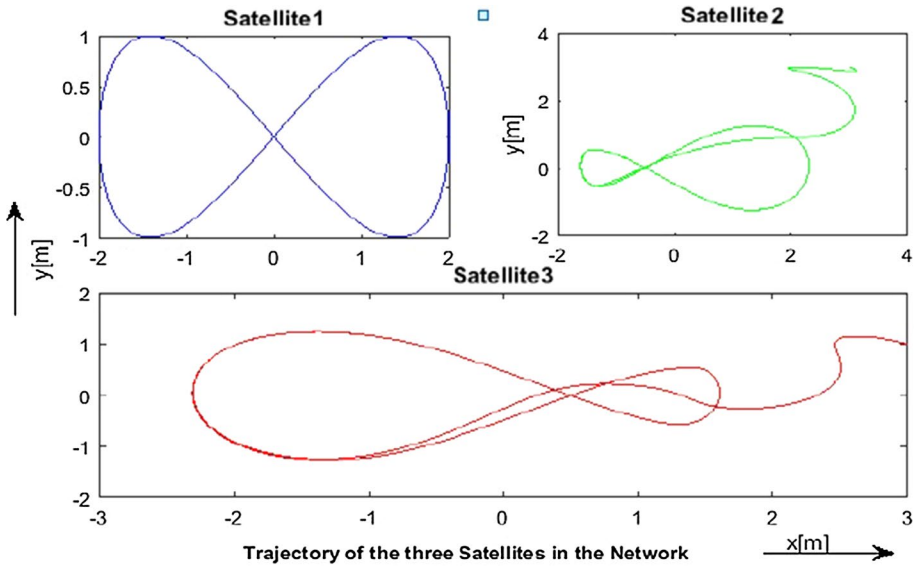**Fig. 7** Cluster formation in PBNT

Fig. 8 Trajectories of the satellites in SBWSN with triangular formation in PBNT

between two satellites is simulated and shown in Figs. 9 and 10 . This deviation is better understood by taking the normalisation of distance of the triangular formation as shown in the Fig. 11

The tracking of satellites position is done periodically to maintain the formation in the network. The periodicity depends on the orbital parameters, convergence time,
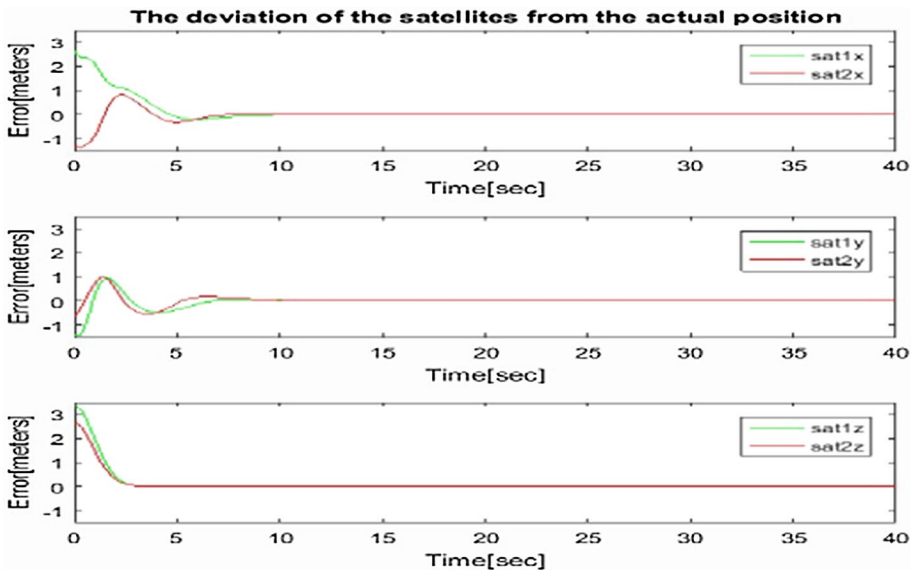

Fig. 9 The deviation of the satellites from the angular position
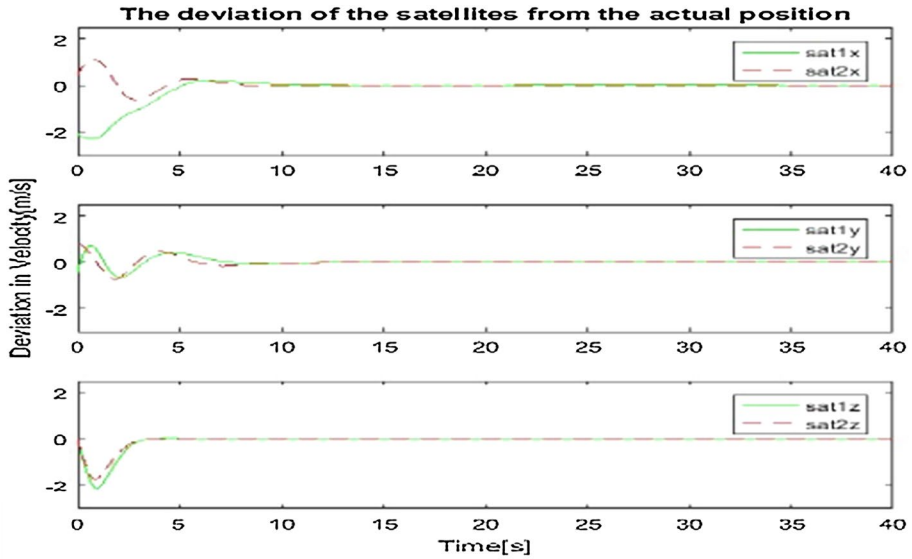
Fig. 10 The deviation of the satellites from the angular velocity
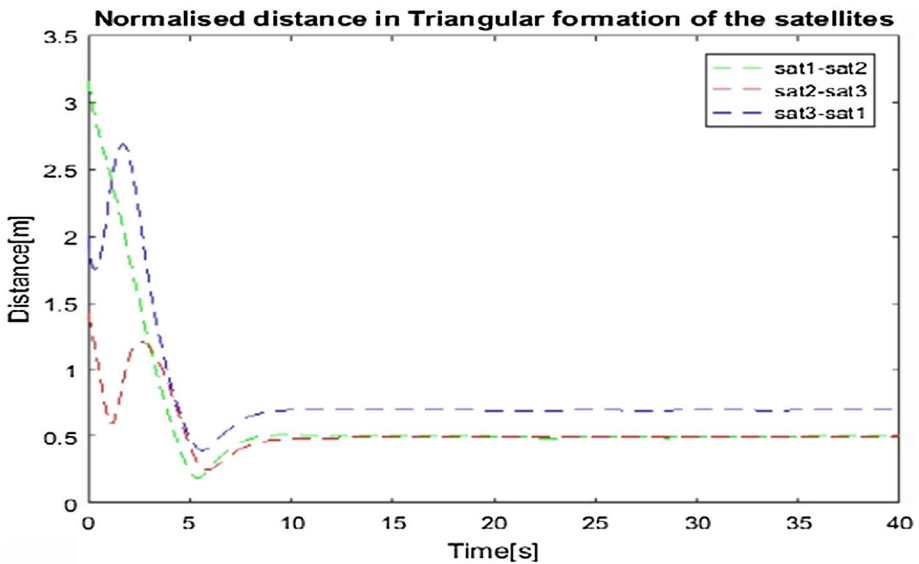
Fig. 11 The normalisation of distance in triangular grid formation

hardware and software capabilities of the satellites in the network. If the periodicity is too long the deviation is more, correction becomes difficult and may lead to mission failure.

The error distance is measured from the desired to the actual position between the two satellites and the error is determined as shown in the Figs. 9 and 10 .

From these simulation one can determine the deviation of each satellite relative to the other in the formation. The amount of time taken to converge to the desired formation is determined by orbital parameters and the capabilities of the ADCS. Till now we saw triangular gird formation and determination of error or deviation from the desired trajectory to have the formation intact.

Scenario 1 Let us consider a simple network as shown in the Fig. 12 and determine the laplaicain matrix and have plotted the eigenvalues using the Gershgorin theorem. The Eq. 74 represent the laplaicain matrix graph where s is the source node, t is target node, A represent the Adjacency matrix. The neighbours in the graph are incident or adjacency matrix. In PBNT, triangular grid form the fundamental component which can further be tiled during dynamic clustering.

$$
\begin{aligned}
s &= [1, 1, 1, 2]; \\
t &= [2, 3, 4, 3]; \\
A &= (2, 1), (3, 1), (4, 1), (1, 2), \\
&\quad (3, 2), (1, 3), (2, 3), (1, 4) \\
L &= \begin{bmatrix} 3 & -1 & -1 & -1 \\ -1 & 2 & -2 & 0 \\ -1 & -1 & 2 & 0 \\ -1 & 0 & 0 & 1 \end{bmatrix}
\end{aligned}
\tag{74}
$$

It becomes important to determine if the topology of the network is stable. In our work we have polygon based network topology forming a fullerence. Hence we determine the stability of network with pentagon followed with the hexagon which are the basic units. The fullerence is formed by these basic units with pentagons and hexagons as shown in the Fig. 7. If these basic unit are stable then the entire network will be stable.

We now consider dynamic cluster formed by pentagon and hexagon graph that forms the fullerence in PBNT. We determine stability of clusters by determining negibhour using adjacency or incident matrix and later find the Laplacian matrix for directed
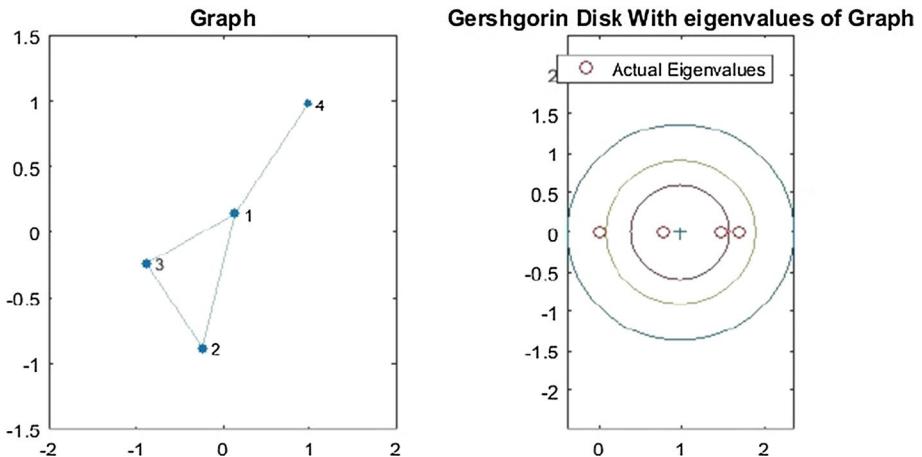

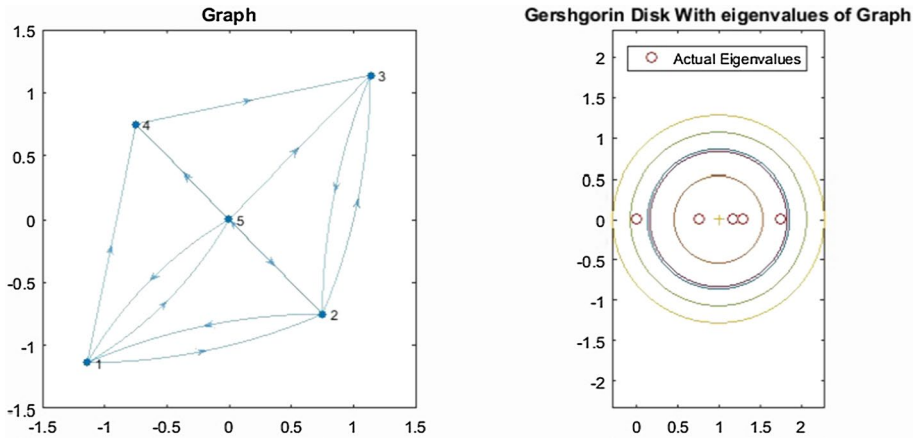**Fig. 12** Dynamic formation of triangulation and its eigenvalues on Gershgorin disk

Fig. 13 Dynamic formation of pentagon graph 1 and its eigenvalues on Gershgorin disk
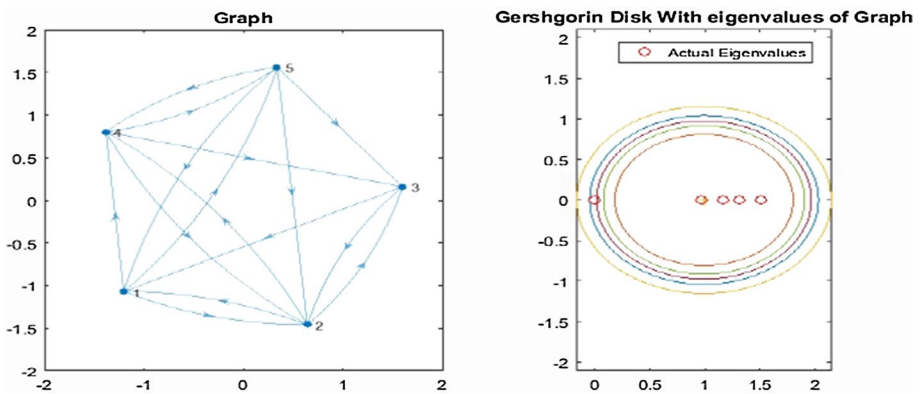

Fig. 14 Dynamic formation of pentagon graph 2 and its eigenvalues on Gershgorin disk

graphs with schur, perrons . The Eqs. 75 to 84 represent dynamic clusters. The results of these are shown in Figs. 13, 14, 15, 16, 17, 18, 19 and 20 respectively.Nyquist criteria is used and also we shown that the clusters are stable as the eigen values lies within radius of one on Gershgorin plot. Hence we say that these dynamic cluster are satble and thus the entire network is stable.

$$
\begin{aligned}
s &= [1, 1, 1, 2, 2, 2, 3, 4, 5, 5, 5, 5]; \\
t &= [2, 4, 5, 1, 3, 4, 2, 3, 1, 2, 3, 4]; \\
A &= (1, 2), (1, 4), (1, 5), (2, 1), (2, 3), \\
&\quad (2, 4), (3, 2), (4, 3), (5, 1), (5, 2), (5, 3), (5, 4)
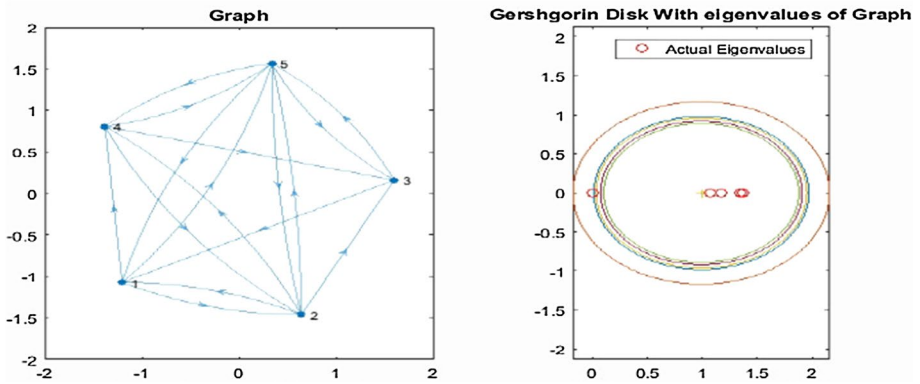\end{aligned}
\tag{75}
$$

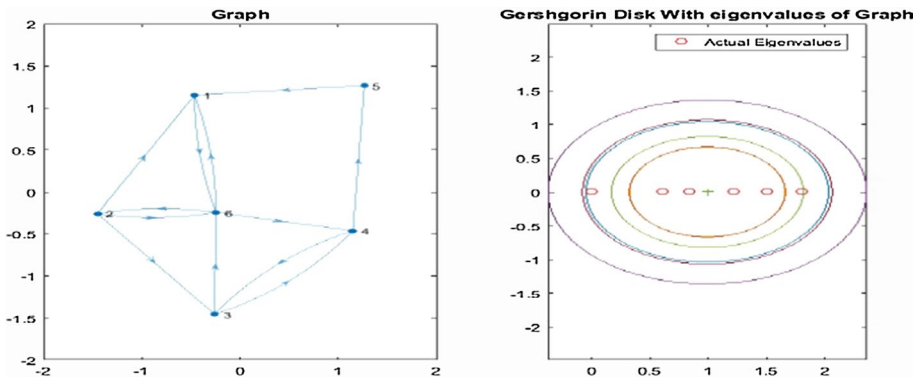**Fig. 15** Dynamic formation of pentagon Graph 2 and its eigenvalues on Gershgorin disk

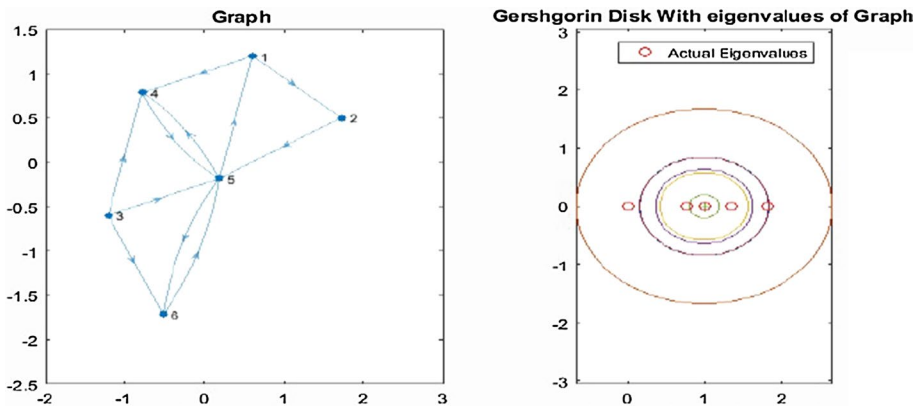**Fig. 16** Dynamic formation of hexagon Graph 1 and its eigenvalues on Gershgorin disk

Fig. 17 Dynamic formation of Hexagon Graph 2 and its eigenvalues on Gershgorin disk
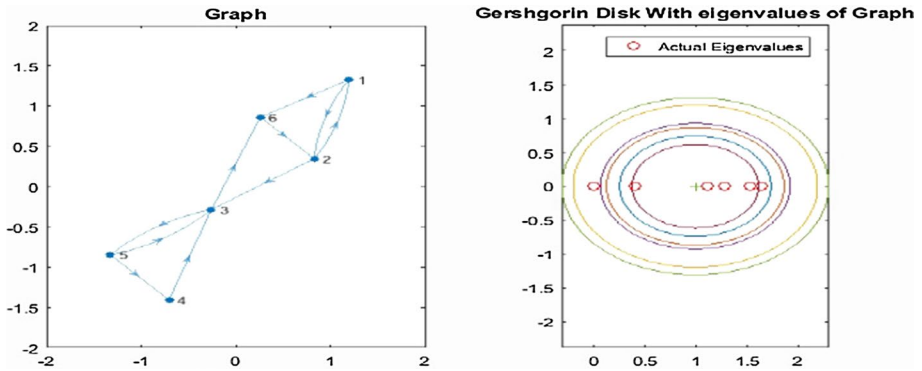
Fig. 18 Dynamic formation of hexagon Graph 3 and its eigenvalues on Gershgorin disk
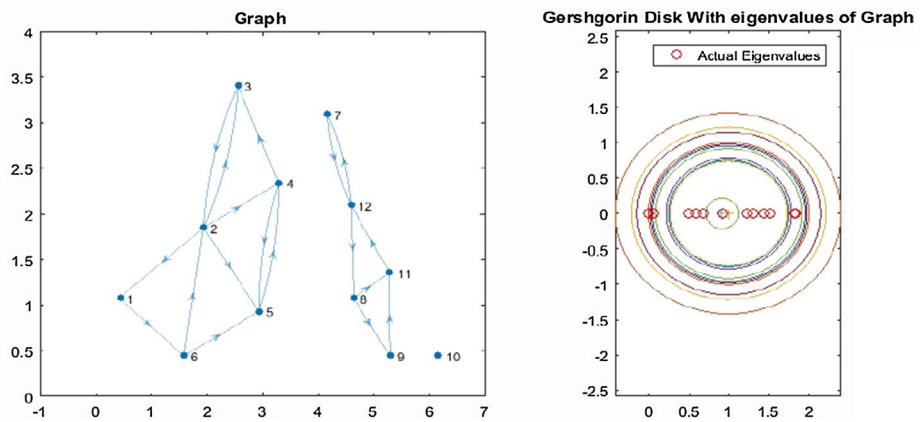

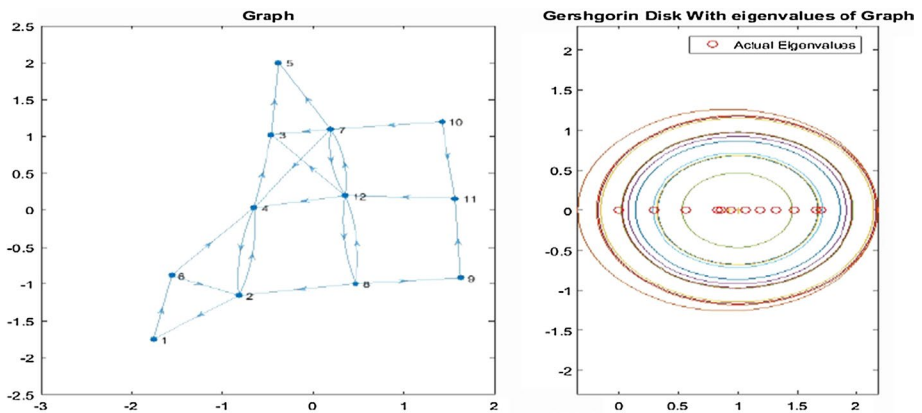**Fig. 19** Dynamic formation of Graph 4 and its eigenvalues on Gershgorin disk

Fig. 20 Concatenation of Graph 4 to another sub-graph during dynamic cluster formation and its eigenvalues on Gershgorin disk

$$s = [1, 1, 1, 2, 2, 2, 3, 3, 4, 4, 4, 5, 5, 5, 5];$$
$$t = [2, 4, 5, 1, 3, 4, 2, 1, 3, 2, 5, 1, 2, 3, 4];$$
$$A = (1, 2), (1, 4), (1, 5), (2, 1), (2, 3), (2, 4), (3, 1), (3, 2),$$
$$(4, 2), (4, 3), (4, 5), (5, 1), (5, 2), (5, 3), (5, 4);$$

(76)

$$s = [1, 1, 1, 2, 2, 2, 2, 3, 3, 4, 4, 4, 5, 5, 5, 5];$$
$$t = [2, 4, 5, 1, 3, 4, 5, 5, 1, 3, 2, 5, 1, 2, 3, 4];$$
$$A = (1, 2), (1, 4), (1, 5), (2, 1), (2, 3), (2, 4), (2, 5),$$
$$(3, 5), (3, 1), (4, 2), (4, 3), (4, 5), (5, 1), (5, 2), (5, 3), (5, 4)$$

(77)

$$s = [1, 2, 2, 2, 3, 3, 4, 4, 5, 6, 6, 6];$$
$$t = [6, 1, 3, 6, 6, 4, 3, 5, 1, 1, 2, 4];$$
$$A = (1, 6), (2, 1), (2, 3), (2, 6), (3, 6),$$
$$(3, 4), (4, 3), (4, 5), (5, 1), (6, 1), (6, 2), (6, 4)$$

(78)

$$s = [1, 1, 2, 3, 3, 3, 4, 5, 5, 5, 6];$$

(79)

$$t = [2, 4, 5, 4, 5, 6, 5, 4, 6, 1, 5];$$

(80)

$$A = (1, 2), (1, 4), (2, 5), (3, 4), (3, 5), (3, 6),$$
$$(4, 5), (5, 4), (5, 6), (5, 1), (6, 5)$$

(81)

$$s = [1, 1, 2, 2, 3, 3, 4, 5, 5, 6];$$
$$t = [2, 6, 1, 3, 6, 5, 3, 3, 4, 2];$$
$$A = (1, 2), (1, 6), (2, 1), (2, 3),$$
$$(3, 6), (3, 5), (4, 3), (5, 3), (5, 4), (6, 2)$$

(82)

$$s = [1, 2, 2, 2, 2, 3, 4, 4, 5, 6, 6, 7, 8, 8, 9, 11, 12, 12];$$
$$t = [6, 1, 3, 4, 5, 2, 3, 5, 4, 2, 5, 12, 9, 11, 11, 12, 7, 8];$$
$$A = (1, 6), (2, 1), (2, 3), (2, 4), (2, 5), (3, 2), (4, 3), (4, 5), (5, 4),$$
$$(6, 2), (6, 5), (7, 12), (8, 9), (8, 11), (9, 11), (11, 12), (12, 7), (12, 8)$$

(83)

$$s = [1, 2, 2, 3, 4, 4, 5, 6, 6, 7, 7, 7, 8, 8, 8, 9, 10, 10, 11, 12, 12, 12, 12];$$
$$t = [6, 1, 4, 5, 2, 3, 5, 4, 2, 5, 3, 4, 12, 2, 9, 11, 7, 11, 12, 07, 08, 04, 03];$$
$$A = (1, 6), (2, 1), (2, 4), (3, 5), (4, 2), (4, 3), (5, 5), (6, 4), (6, 2),$$
$$(7, 5), (7, 3), (7, 4), (8, 12), (8, 2), (8, 9), (9, 11), (10, 7), \quad (84)$$
$$(10, 11), (11, 12), (12, 07), (12, 08), (12, 04), (12, 03)$$

These are few examples of dynamic clustering of satellites based on the adjacency and Incident matrix. Thus from the above examples we show that the PBNT is stable, while maintaining the formation stability.

5 Conclusions

The work in this paper present the method to represent the small satellite network in a topology and maintain its stability in formation using the trajectories. The trajectories are determined using covariant derivatives and stability is derived using local distance(angular distance and angular velocity) between the neighbours of satellites in the network. The error in the formation is determined and corrected using underlying ADCS to have rigid formation of the network topology. The method to determine if the topology is stable, interconnections between the satellites/nodes during dynamic cluster formation has to be stable as these satellites are mobile in space. In this work, we have used graph theory as it provides the insight of its interconnections during tiling used for dynamic cluster formations. This also provides necessary information of actual position and the relative positions in the network. This work becomes a prerequisite method to determine the available paths/ routes that is essential for routing the data from one node to other, for information gathering and aggregation in SBWSN.

References

1. Twiggs, R. J. (2000). A new generation of picosatellite for education and industry low-cost space experimentation. In *AIAA/USU small satellite conference proceedings V-5, 2000.*
2. Zhou, D., & Schwager, M. (2015). Virtual rigid bodies for coordinated agile maneuvering of teams of micro aerial vehicles. In *2015 IEEE international conference on robotics and automation (ICRA), Seattle, WA* (pp. 1737-1742). https://doi.org/10.1109/ICRA.2015.7139422.
3. Mehrjerdi, H., Ghommam, J., & Saad, M. (2011). Nonlinear coordination control for a group of mobile robots using a virtual structure. *Mechatronics, 21*(7), 1147–1155.
4. Balch, T., & Arkin, R. C. (1998). Behavior-based formation control for multirobot teams. *IEEE Transactions on Robotics and Automation, 14*(6), 926–939. https://doi.org/10.1109/70.736776.
5. McLaughlin, C. A., Sabol, C., Swank, A., Burns, R. D., & Luu, K. K. (2002). Modeling relative position relative velocity and range rate for formation flying. Air Force Research Lab Kirtland AFB NMSPACE Vehicles Directorate.
6. Earl, M. A. (2006). Determining the orbital height of a low-earth-orbiting artificial satellite observed near the local zenith. *Journal of the Royal Astronomical Society of Canada, 100,* 199.
7. Crouch, P., & Leite, F. S. (1995). The dynamic interpolation problem: On Riemannian manifolds, Lie groups, and symmetric spaces. *Journal of Dynamical and Control Systems, 1*(2), 177–202.
8. Lafferriere, G., Williams, A., Caughman, J., & Veerman, J. J. P. (2005). Decentralized control of vehicle formations. *Systems & Control Letters, 54*(9), 899–910.
9. Kuruba, P., & Sutagundar, A. V. (2017). Emerging trends of space-based wireless sensor network and its applications. In N. Kamila (Ed.), *Handbook of research on wireless sensor network trends,*

technologies, and applications (pp. 35–57). IGI Global. https://doi.org/10.4018/978-1-5225-0501-3.ch002.

10. Gioioso, G., Franchi, A., Salvietti, G., Scheggi, S., & Prattichizzo, D. (2014). The flying hand: A formation of UAVs for cooperative aerial tele-manipulation. In *2014 IEEE international conference on robotics and automation (ICRA), Hong Kong* (pp. 4335–4341). https://doi.org/10.1109/ICRA.2014.6907490.

11. Waharte, S., Trigoni, N., & Julier, S. (2009). Coordinated search with a swarm of UAVs. In *2009 6th IEEE annual communications society conference on sensor, mesh and ad hoc communications and networks workshops, Rome* (pp. 1–3). https://doi.org/10.1109/SAHCNW.2009.5172925.

12. Kuo, B. C., & Golnaraghi, F. (2003). *Automatic control systems*. McGraw-Hill Education.

13. Karnopp, D. C., Margolis, D. L., & Rosenberg, R. C. (2012). *System dynamics: Modeling, simulation, and control of mechatronic systems*. Wiley.

14. Ogren, P., Fiorelli, E., & Leonard, N. E. (2004). Cooperative control of mobile sensor networks: Adaptive gradient climbing in a distributed environment. *IEEE Transactions on Automatic Control, 49*(8), 1292–1302.

15. Navabi, M., Barati, M., & Bonyan, H. (2013). Algebraic orbit elements difference description of dynamics models for satellite formation flying. In *2013 6th international conference on recent advances in space technologies (RAST)* (pp. 277–280). IEEE.

16. Massari, M., & Zamaro, M. (2014). Application of SDRE technique to orbital and attitude control of spacecraft formation flying. *Acta Astronautica, 94*(1), 409–420.

17. Kuruba, P., Sutagundar, A. V. (2017). Space based wireless sensor network: a survey, internet of things and cloud computing. *Special Issue: Advances in Cloud and Internet of Things, 5*(5–1), 19–29. https://doi.org/10.11648/j.iotcc.s.2017050501.14.

18. Kuruba, P., & Dusyantha, N. D. (2020). Polygon based topology formation and information gathering in satellite based wireless sensor network. *Wireless Personal Communication*. https://doi.org/10.1007/s11277-020-07568-9.

19. Reinhard Diestel. (2017). *Graph Theory* (5th. ed.). Springer Publishing Company, Incorporated.

20. Chung, F. (2005). Laplacians and the Cheeger inequality for directed graphs. *Annals of Combinatorics, 9*(1), 1–19.

21. Chung, F. R., & Graham, F. C. (1997). *Spectral graph theory (No. 92)*. American Mathematical Soc.

22. Merris, R. (1994). Laplacian matrices of graphs: A survey. *Linear Algebra and its Applications, 197,* 143–176.

23. Mohar, B., Alavi, Y., Chartrand, G., & Oellermann, O. R. (1991). The Laplacian spectrum of graphs. *Graph Theory, Combinatorics, and Applications, 2*(871–898), 12.

24. Selva, D., & Krejci, D. (2012). A survey and assessment of the capabilities of Cubesats for Earth observation. *Acta Astronautica, 74,* 50–68.

Padmaja Kuruba holds a Bachelor degree in Electronics and Communication Engineering and Master in Technology in Digital Electronics. She has over 18 years of experience including Industry and Academia. She has worked with Larsen and Tubro (L&T) InfoTech, Cisco system, Mindtree Limited and Kyocera Wireless Limited. She has worked at Jain University Bengaluru and currently is associated with Global Academy of Technology Bengaluru. Her area of research includes Wireless Communication (LTE and Wimax), Wireless Sensor Networks, Satellite Communication. She has been awarded with Excellent Performer Award at L&T (Larsen and Tubro InfoTech) for LTE Project, Shining Star award from Mindtree, Certified with 'A' Grade for Wireless and Mobile Communication at Indian Institute of Science (IISC) Bengaluru. She has filed a Patent on Navigation System. She is Recognized as Scientific Researcher. She was designated as Board of Examination at Jain University. She has won prizes at several National and State Level Project Competition. She is also a Resource person at National Level, Faculty Development Programs. She has contributed

to the research field by authoring few conference and journal papers. She has also authored a Book Chapter in "Handbook of Research on Wireless Sensor Network Trends, Technologies, and Applications".

N. D. Dushyantha holds a M.Tech. degree and a Ph.D. in Electronics and Communication Engineering. He is currently a professor at K S School of Engineering and Management, Bangalore, His research interests include Speech processing, Machine learning, Deep learning. He is author or co-author of over 20 international journal papers or conference proceedings.